Journal of the Serbian Chemical Society
JSCS@tmf.bg.ac.rs • www.shd.org.rs/JSCS
J. Serb. Chem. Soc. *88* (12) 1223–1236 (2023)
JSCS–5691
Original scientific paper
Published 19 December 2023

Ligands containing 7-azaindole functionality for inner-sphere hydrogen bonding: Structural and photophysical investigations

ALEC B. COLES, OSKAR G. WOOD and CHRIS S. HAWES*

School of Chemical and Physical Sciences, Keele University, Keele ST5 5BG, United Kingdom

(Received 23 June, revised 10 July, accepted 8 September 2023)

Abstract: The synthesis, structural analysis and spectroscopic characterisation of three new 7-azaindole ligands is reported, alongside a novel 7-azaindole derived coordination polymer, with the aim of identifying new bridging ligands containing inner-sphere hydrogen bond donor functionality. Structural characterisation shows that the 7-azaindole hydrogen bond donor ability is significantly stronger in the hydrazone and imine species **1** and **2** compared to the amine **3**, with the opposite trend evident in their hydrogen bond acceptor character. These findings are mirrored by the fluorescence spectroscopy results which show bimodal emission, characteristic of multiple emissive species related by proton transfer, is only evident in the amine species and not the more acidic imines. The polymeric copper(II) complex of the hydrazone ligand **1** shows the anticipated inner-sphere hydrogen bonding with a similar donor strength to that observed in the free ligand, which leads to deformation in the remainder of the coordination sphere. These results show the untapped versatility of the 7-azaindole functional group as a building block for ligands in coordination polymers and other multinuclear assemblies, with the potential for both stabilisation through hydrogen bonding and interesting photophysical properties.

Keywords: coordination chemistry; X-ray crystallography; Schiff bases; fluorescence spectroscopy.

INTRODUCTION

In the development of new functional coordination compounds, careful and deliberate ligand design is essential for balancing geometry and functionality.[1] In this regard, synthetic routes which allow access to a broad range of ligand functionalities are useful for fine-tuning properties of the resulting coordination compounds.[2,3] The Schiff base functionality is useful for these purposes, as simple aldehyde and amine precursors can be used to self-assemble ligands (or libraries of ligands) and coordinate to metal ions *in situ*.[4,5] Schiff base complexes, and

* Corresponding author. E-mail: c.s.hawes@keele.ac.uk
https://doi.org/10.2298/JSC230623061C

those of related hydrazone and semicarbazide functionalities,[6,7] have been widely explored for catalysis, medicine, molecular magnetism and sensing applications, among others.[8–12] These complexes often suffer from relatively low stability in the presence of water and other nucleophiles, however, which despite providing interesting possibilities for reversible self-assembly[13] can also limit their use in aqueous environments. As such, the inclusion of extra stabilising interactions around the coordination sphere may be a viable strategy for the generation of new stable Schiff base complexes.

Our interest in this area has concerned nitrogen heterocyclic ligands with hydrogen bond donors near the metal ion.[14] Such species may strengthen the coordination sphere against chemical degradation, both through the enthalpic contribution of extra bonding interactions but also by restricting molecular rotation or rearrangement.[15,16] The *1H*-pyrazole moiety is the quintessential example of such a ligand, and many instances of hydrogen-bonded assemblies in pyrazole--containing complexes are known.[17–19] However, expansion of this approach to larger or fused heterocycles is less common.[20] The 7-azaindole (7AI) fragment shows similar structural characteristics to *1H*-pyrazole in this regard. As shown in Fig. 1, 7AI contains a heterocyclic N–H hydrogen bond donor (with similar acidity to pyrazole) separated by one carbon to an imine-like nitrogen atom, and with a carbon backbone readily capable of derivatisation to add additional metal coordination sites. The photophysics of the parent heterocycle have been widely studied based on the tendency for solvent-dependent excited state proton transfer in the dimer and solvent adducts,[21–23] and as a simplified structural analogue for DNA base pairs.[24] Despite the interest in these compounds, surprisingly there have been relatively few investigations into the coordination chemistry of 7AI ligands in polymeric species, mostly focused on N-substituted derivatives.[25–27] Here we describe our attempts to develop heterotopic 7AI ligands, investigations into their photophysical behaviour, and report an unusual structurally characterised example of a 7AI-based coordination polymer.

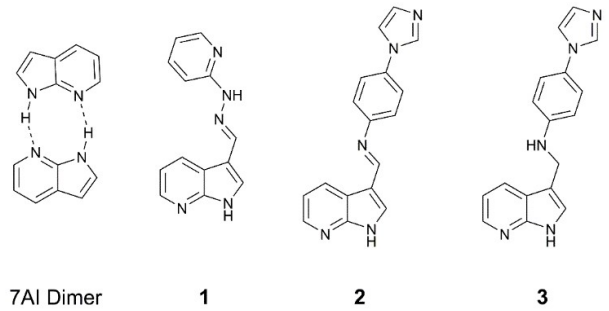

Fig. 1. Compounds of interest to this study; the 7-azaindole hydrogen-bonded dimer represented as the ground-state tautomer (7AI Dimer), and the structures of compounds **1**–**3**.

EXPERIMENTAL

Materials and methods

All starting materials and reagents were purchased from Merck or Fluorochem. NMR spectra were collected using a Bruker Avance III HD spectrometer using DMSO-d_6 and referenced to the residual solvent peak. Infrared spectra were recorded on a Thermo Fisher Nicolet iS10 spectrometer with an ATR sampling attachment. Elemental analysis was performed on a Thermo Flash 2000 CHNS elemental analyser. Photophysical measurements were collected using an Agilent Cary 60 Bio spectrophotometer and an Agilent Cary Eclipse fluorimeter using Starna quartz cuvettes of 1 cm path length. X-ray powder diffraction patterns were collected using a Bruker D8 Advance diffractometer with CuKα (λ = 1.5406 Å) radiation. Samples were mounted on a zero background silicon sample holder, and measured in the range 5–55° (2θ). Single crystal X-ray diffraction methods, as well as analytical and spectral data, are given in the Supplementary material to this paper. Hydrogen bonding parameters are given in Table I.

TABLE I. Hydrogen bonding parameters for all structures; symmetry codes: [1]1–*x*,–1/2+*y*,3/2–*z*; [2]2–*x*,–1/2+*y*,1/2–*z*; [3]–1–*x*,1–*y*,1–*z*; [4]1–*x*,1–*y*,–*z*; [5]+*x*,+*y*,–1+*z*; [6]1/2–*x*,1–*y*,1/2+*z*; [7]3/2–*x*,1–*y*,1/2+*z*

D–H···A	*d*(D–H) / Å	*d*(H–A) / Å	*d*(D–A) / Å	D–H–A / °
Compound **1**				
N2–H2···N5[1]	0.897(17)	1.977(18)	2.868(3)	173(3)
N7–H7···N10[2]	0.902(17)	1.946(18)	2.840(3)	171(3)
Compound **2**				
N2–H2···N1[3]	0.914(18)	1.958(19)	2.865(4)	171(3)
Compound **3**				
N2–H2···N1[4]	0.895(15)	2.054(16)	2.933(2)	167(2)
N3–H3···N5[5]	0.889(16)	2.104(16)	2.990(2)	174(2)
Poly-[Cu(**1**)Cl_2]				
N2–H2···Cl2[6]	0.88(2)	2.39(3)	3.225(4)	157(4)
N4–H4···Cl1[7]	0.89(2)	2.56(3)	3.380(3)	154(4)

*Synthesis of 7-azaindole-3-carboxaldehyde 2-pyridylhydrazone (**1**)*

To a suspension of 7-azaindole-3-carboxaldehyde (243 mg, 1.66 mmol) in 25 mL of methanol was added 2-hydrazinopyridine (183 mg, 1.67 mmol), and the mixture was heated under reflux for 24 hr. On cooling to room temperature an orange precipitate formed which was isolated by filtration, washed with methanol and dried in air. Yield 210 mg (53 %).

*Synthesis of 7-azaindole-3-carboxaldehyde 4-(*N*-imidazolyl)phenyl imine (**2**)*

To a suspension of 7-azaindole-3-carboxaldehyde (549 mg, 3.76 mmol) in MeOH (25 mL) was added 4-(*N*-imidazolyl)aniline (597 mg, 3.74 mmol), and the mixture was heated under reflux for 24 h. On cooling to room temperature, the resulting off-white precipitate was filtered, washed with cold methanol and air dried. Yield 559 mg (52 %).

*Synthesis of 3-(4-(*N*-imidazolyl)phenyl)aminomethyl-7-azaindole (**3**)*

To a suspension of compound **2** (540 mg, 1.88 mmol) in MeOH (50 mL) was added $NaBH_4$ (160 mg, 4.22 mmol) portion-wise over 30 min. Following this addition, the mixture was stirred at room temperature overnight. After 24 h, the solution was poured onto ice water

(15 mL) and the white precipitate was isolated by filtration, washed with a 1:1 MeOH:H_2O mixture, and dried in air. Yield 486 mg (89 %).

*Synthesis of poly-[Cu(**1**)Cl_2]*

A suspension of **1** (11 mg, 46 μmol) in methanol (5 mL) was combined with a solution of copper(II) chloride dihydrate (7.0 mg, 41 μmol) in methanol (5 mL). The resulting dark brown solution was dispersed by sonication for 10 min before being filtered, and the filtrate was subjected to diffusion of diethyl ether vapour. Dark brown crystals were formed within 24 h, isolated by filtration and washed with a small amount of cold methanol. Yield 8.5 mg (56 %).

RESULTS AND DISCUSSION

The synthesis of the 7AI derivatives **1** and **2** was achieved in a single step condensation reaction from 7-azaindole-3-carboxaldehyde and 2-hydrazinopyridine or *N*-(4-aminophenyl)imidazole, respectively. Reduction of **2** with sodium borohydride afforded the amine derivative **3** in good yield. These ligands, shown in Fig. 1, were chosen for a study into the effect of backbone substitution on the coordination chemistry and photophysics of 7AI derivatives, based on their potential for bridging coordination through the additional heterocyclic groups. Single crystals of all three ligands were first analysed by single crystal X-ray diffraction to determine their geometric parameters and tendencies for hydrogen bonding in the absence of metal ions.

Single crystals of **1** were prepared by recrystallization from ethanol, and the diffraction data were solved and refined in the monoclinic space group $P2_1/c$ with $Z' = 2$. The two residues in the asymmetric unit vary only slightly in their molecular geometry. Both residues adopt the expected *E* configuration at the hydrazone and essentially coplanar *anti* conformations for the terminal pyridine rings, with N_{PY}–C–N(H)–N torsion angles of 178.7(2) and 169.5(2)° for residues **1** and **2**, respectively, as shown in Fig. 2. A slight difference is also observed in the azaindole···pyridine interplanar angles for the two residues, of 10.6 *vs.* 12.8°, respectively.

The *anti* conformation of the pyridylhydrazone in **1** results in both this group and the 7AI moiety adopting equivalent hydrogen bond donor/acceptor capabilities. Interestingly, the hydrogen bonding mode observed for both residues is a head-to-tail interaction between one 7AI group and one pyridylhydrazone group, rather than the more symmetric head-to-head/tail-to-tail pairing. Generally, formation of the strongest donor/acceptor pair is expected, followed by the next strongest, although this can be complicated by many structural factors.[28] While unsubstituted 7AI has a higher ground state pKa than typical pyridylhydrazones (12.1 *vs.* 10–11, respectively),[29,30] we would anticipate the electron withdrawing substituent at the 7AI 3-position to bring these two values closer to unity. However, the difference in geometry for the resulting $R_2^2(8)$ rings[31] presumably disfavours the symmetric dimer which is observed in simpler 7AI systems.[32] Here, the idealised N–H vector is 18° removed from the acceptor lone pair in 7AI,

compared to these vectors being parallel in the pyridylhydrazone (as with other hydrogen bond dimers, such as carboxylic acids).[33] The difference in hydrogen bond donor strength is evident from the difference in donor···acceptor distances, which fall at 2.869(3) and 2.840(3) Å for the 7AI donors and 3.048(3) and 3.195(3) Å for the hydrazone donors. These hydrogen bonds between molecules lead to two crystallographically independent, parallel hydrogen bonding chains oriented parallel to the *b* axis. These chains further interact through π···π contacts which, as expected, take a head-to-tail form to favour contact between the relatively electron rich and poor regions of the two aromatic systems.

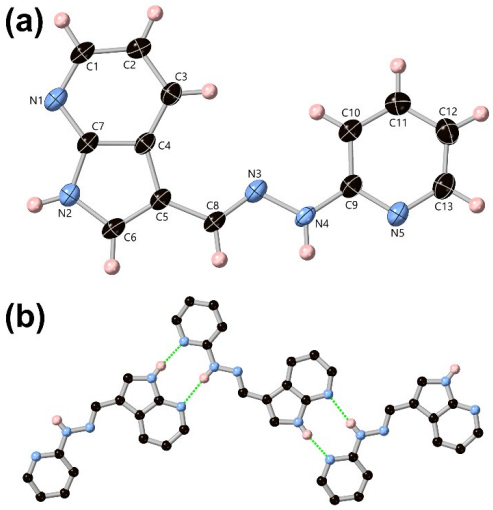

Fig. 2. a) Structure of compound **1** with atom labelling scheme. ADPs are rendered at the 50 % probability level, and the second fragment is omitted for clarity. b) The hydrogen bonding behaviour of compound **1**. Selected hydrogen atoms are omitted for clarity.

Single crystals of compound **2** were isolated from ethanol, and the diffraction data were solved and refined in the monoclinic space group $P2_1/n$ with $Z' = = 1$. The structural model confirms the expected structure as shown in Fig. 3, showing the *E* configuration of the imine and an essentially coplanar shape, with the central phenyl ring exhibiting mean interplanar angles of 6.3 and 23.8° relative to the 7AI and imidazole groups, respectively. With only one classical hydrogen bond donor, the centrosymmetric 7AI dimer motif is observed with an N···N distance of 2.865(4) Å equivalent to the 7AI-donated interactions seen in **1**, and N–H···N angle of 171(3).° Neither the imine nor imidazole nitrogen atoms participate in any significant directional interactions with other hydrogen atoms. The dominant modes of intermolecular interaction beyond hydrogen bonding are edge-to-face C-H···π contacts between the imidazole and 7AI groups. The shortest interatomic distances of 3.532(5) and 3.544(5) Å for C17···C3 and C6···C15, respectively, are consistent with typical magnitudes for such interactions.[34]

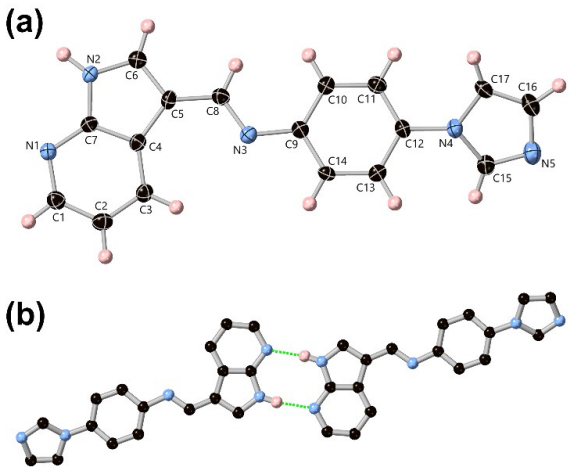

Fig. 3. a) Structure of compound **2** with atom labelling scheme. ADPs are rendered at the 50 % probability level. b) Hydrogen bonding behaviour in the structure of **2** consisting of a centrosymmetric 7AI dimer-type motif. Selected hydrogen atoms are omitted for clarity.

For comparison with additional hydrogen bond donation capability, and to provide a spectroscopic comparison with a more electron rich 7AI derivative, compound **2** was reduced to the amine **3**, which was crystallised from ethanol. The diffraction data for **3** were solved and refined in the monoclinic space group $P2_1/n$, with $Z' = 1$. Reduction to the amine is evident from the longer C–N bond (1.446(3) Å, *cf.* 1.285(4) Å in **2**) and a significantly less planar geometry, with the 7AI···phenyl interplanar angle increasing to 66.9°, while the imidazole–phenyl interplanar angle remains similar at 34.4°. The centrosymmetric 7AI dimer hydrogen bonding motif is again evident, as shown in Fig. 4, although reduction to the amine leads to a much longer N···N distance of 2.933(2) Å, while the N–H···N angle is unchanged at 167(2)°. The longer donor···acceptor distance in this interaction likely relates to lower acidity of the N–H group following loss of the electron withdrawing imine. This is supported by the infrared spectra for the three ligands. Compounds **1** and **2** show similar broad absorbances at 3205 and 3210 cm^{-1}, respectively, consistent with the NH stretch in a hydrogen-bonded 7AI species.[35] In **3**, this band is shifted to a higher frequency of 3247 cm^{-1} indicative of a decrease in hydrogen bond donor strength for this species in the solid state.

In addition to the 7AI dimer, further hydrogen bonding is evident between the amine N–H group and the imidazole nitrogen atom of adjacent molecules, at a similar donor···acceptor distance of 2.990(2) Å and N–H···N angle of 174(2)°. The combination of both interactions leads to the formation of a one-dimensional hydrogen bonded ribbon oriented parallel to the *c* axis. Adjacent ribbons interact

through a series of diffuse π···π and C–H···π contacts, although these are less prominent than those in **2** due to the lesser degree of conjugation in **3**.

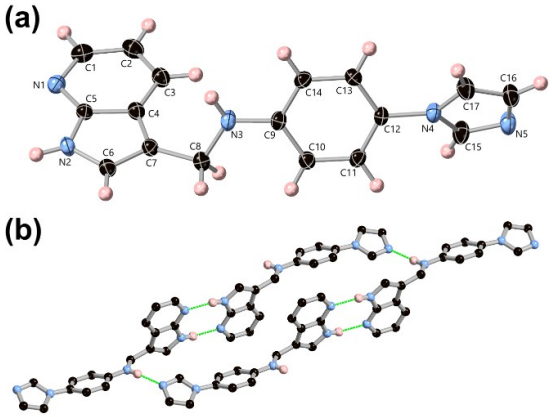

Fig. 4. a) Structure of compound **3** with atom labelling scheme. ADPs are rendered at the 50 % probability level. b) The hydrogen bonding environment in the structure of **3**. Selected hydrogen atoms are omitted for clarity.

With the structures and key interaction modes of **1**–**3** confirmed, we turned our attention to their use as ligands for coordination compounds. Despite our efforts over a range of conditions (near-ambient to high temperature hydro/solvothermal), we were unable to isolate any coordination compounds containing ligands **2** or **3**, instead generally recovering either unreacted starting materials or unidentified decomposition products. We ascribe these to the poor solubility of these species and vulnerability to either hydrolysis (**2**) or acid catalysed amine elimination (**3**)[36] reactions at high temperatures, alongside low stability constants for the pure monodentate coordination modes. However, the chelating ligand **1** readily reacted with copper(II) chloride dihydrate at room temperature, to form a dark brown solution giving crystals on standing overnight or under diffusion of diethyl ether vapour, which analysed for a complex of the formula poly-[Cu(**1**)Cl_2], a one-dimensional coordination polymer. The diffraction data for poly-[Cu(**1**)Cl_2] were solved and refined in the orthorhombic space group $P2_12_12_1$ with $Z' = 1$. The copper ion adopts a distorted square pyramidal coordination geometry (τ_5 = = 0.22),[37] where the basal plane is occupied by two *cis*-oriented chlorido ligands and the chelating pyridylhydrazone moiety, while the axial position is occupied by the 7AI nitrogen atom, as shown in Fig. 5. The axial Cu–N distance of 2.293(4) Å is significantly longer than those corresponding to the pyridine or hydrazone nitrogen atoms (2.008(3) and 2.037(3) Å, respectively, a consequence of the typical axial bond elongation in square pyramidal d^9 complexes rather than being indicative of any particular difference in donor strength. The copper ion

acts as a corner in the expanded structure, relating each ligand segment to the next by a mean interplanar angle of 86.6° as the overall zig-zag polymer aligns parallel to the *c* axis.

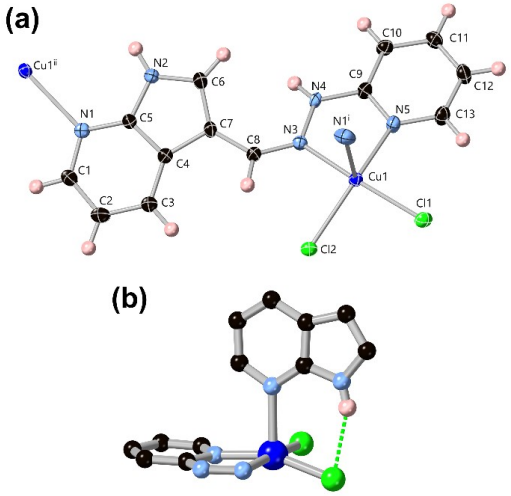

Fig. 5. a) Structure of poly-[Cu(**1**)Cl_2] with atom labelling scheme. ADPs are rendered at the 50 % probability level. Symmetry codes used to generate equivalent atoms: (*i*) ½–*x*, 1–*y*, 1/2+*z*; (*ii*) ½–*x*, 1–*y*, –1/2–*z*. b) The inner-sphere hydrogen bond in the structure of poly-[Cu(**1**)Cl_2] showing the deflection of the chlorido ligand. Selected atoms are omitted for clarity.

The complex poly-[Cu(**1**)Cl_2] contains two classical hydrogen bond donors, and each engages in the expected N–H···Cl hydrogen bonding, given all other acceptors are involved in coordination to the metal ion. As we had intended, the 7AI hydrogen bond donor engages in hydrogen bonding within the coordination sphere to the adjacent chlorido ligand Cl2, at an N···Cl distance of 3.225(4) Å and a relatively small N–H···Cl angle of 157(4)°. The donor···acceptor distance for this interaction is comparable to that typically observed for N–H···Cl contacts (3.2–3.3 Å),[38] and accounting for the *ca.* 0.35 Å difference in atomic radii for N and Cl, are consistent with the donor strength of this group observed in the structure of the free ligand. Notably, the chlorido ligand involved in this interaction is also bent out of the basal plane, evident by the angle N5–Cu1–Cl2 of 159.22(9) (Fig. 5b), compared to the N3–Cu1–Cl1 angle of 172.47(9). The hydrazone N–H group is oriented away from the coordination sphere, and instead donates a hydrogen bond to the chlorido ligand Cl1 of an adjacent chain, as shown in Fig. 6. The longer N···Cl distance of 3.380(4) and N–H···Cl angle of 154(4)° are consistent with the previous observation of a weaker hydrazone N–H donor com-

pared to 7AI. The inter-strand hydrogen bonding also facilitates additional π···π interactions between hydrogen bonded strands, where 7AI and pyridylhydrazone groups interact with a minimum interatomic distance of 3.223(6) Å for C1···C6 and a mean interplanar angle of 18.4°.

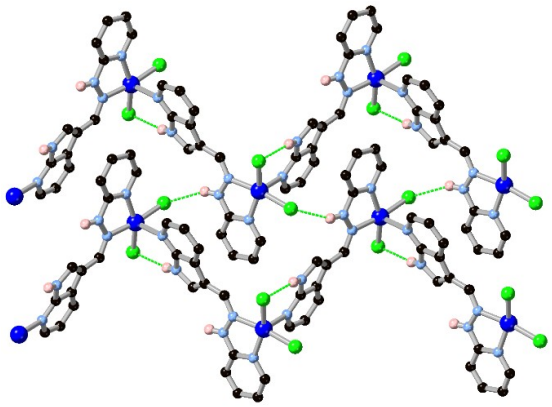

Fig. 6. The extended structure of the coordination polymer *poly*-[Cu(**1**)Cl_2] showing the hydrogen bonding behaviour between strands. Selected hydrogen atoms are omitted for clarity.

The structural data for compounds **1**–**3** suggest reduction of the imine at the 3 position leads to a decrease in hydrogen bond donor strength for the 7AI proton. Given the tendency for the photophysical properties of 7AIs to be impacted by proton transfer, we investigated the absorption and emission behaviour of compounds **1–3** to probe this influence. In DMSO, all three compounds show absorption bands with maxima in the range 22–26×10^3 L mol^{-1} cm^{-1} from n→π* and/or π→π* transitions, as shown in Fig. 7. The more conjugated species **1** and **2** show lower energy absorbances at 325 and 331 nm, respectively, both with higher energy shoulders. The absorbance for **3** has a maximum at 277 nm, with any structuring at the high energy edge falling outside of the solvent window. Excitation leads to emission in the near-UV to visible region of the spectrum; compound **1** shows a single emission band with maximum at 457 nm, while the emission from compound **2** is substantially blue-shifted to 378 nm. Given the similar absorbance profiles and structures of the two compounds, this difference in Stokes shift (8900 *vs*. 3800 cm^{-1}) is surprising, and may indicate the emissive states in the two species arise from different tautomers or hydrogen-bonded environments.

Compound **3**, on the other hand, shows a structured emission profile in DMSO comprised of two bands, the larger at 470 nm with a distinct second band visible as a shoulder at 365 nm. These band positions are similar to those observed for 7-azaindole itself in protic solvents, where the “normal” emission at

370 nm is accompanied by a tautomer band at 510 nm.[39] In contrast to the emission profile here, the normal emission is usually more intense than the tautomer band, although this trend can be reversed in solutions of more acidic alcohols where emission from either the solvated tautomer or protonated cation can be favoured.[40]

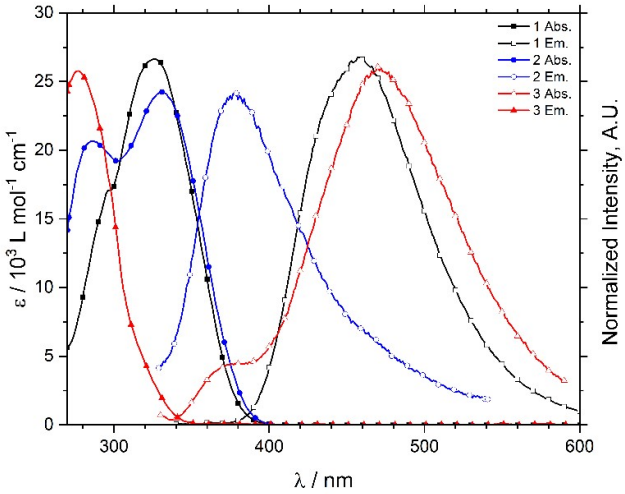

Fig. 7. Combined absorption (solid markers) and normalized emission (hollow markers) spectra for compounds **1** (black, 27 μM, λ_{ex} = 318 nm), **2** (blue, 22 μM, λ_{ex} = 286 nm) and **3** (red, 26 μM, λ_{ex} = 300 nm) in DMSO.

To further explore the discrepancy in emission behaviour of the three 7AI species, each was diluted into acetonitrile, as a weaker hydrogen bond acceptor less likely to mediate proton transfer, and methanol, expected to alter any proton transfer pathways by the formation of hydrogen-bonded solvent adducts. In acetonitrile, all three compounds display essentially equivalent behaviour to that in DMSO with only minor blue-shifting of the emission of all three compounds, indicating slightly negative solvatochromism (Supporting Information). In methanol, however, while compounds **1** and **2** exhibit the same behaviour (albeit at much lower intensity, presumably due to extra vibrational relaxation with solvent protons), the two emission bands in **3** are swapped in intensity, with emission from the normal band at 368 nm much brighter than emission from the tautomer band at 525 nm, as shown in Fig. 8. These findings suggest that only **3,** lacking conjugation at the 3 position, follows the typical excited state proton transfer pathway of the parent 7-azaindole, while the fully conjugated **1** and **2** show emission behaviour which is mostly invariant to the local hydrogen bonding environment. This effect may relate to competition in electronic demand from the imine/

/hydrazone substituent raising the energy of the proton transfer processes, or additional decay pathways involving the backbone, such as photoinduced electron transfer (PET) depopulating the emissive states.

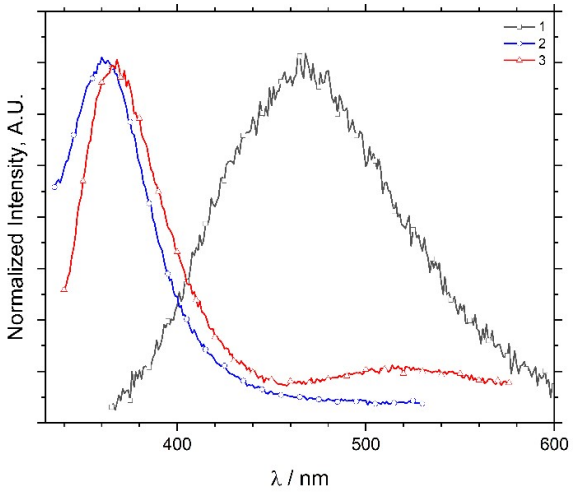

Fig. 8. Normalized emission spectra for compounds 1 (black, 27 μM, λ_{ex} = 318 nm), **2** (blue, 22 μM, λ_{ex} = 280 nm) and **3** (red, 26 μM, λ_{ex} = 300 nm) in MeOH.

CONCLUSION

Three new 7-azaindole derived ligands have been prepared and characterised, and used to generate a crystalline coordination polymer containing a 7-azaindole ligand. Structural analysis of the ligands shows the typical 7AI dimer motif can be overridden in the presence of a more basic acceptor of similar donor–acceptor geometry, while reduction from the imine to the amine significantly reduces the donor capability of the N–H group. On reaction with copper(II), the chelating hydrazone derivative **1** forms a linear coordination polymer containing an inner-sphere hydrogen bonding motif, although likely due to the geometric mismatch of donor and acceptor in this system this interaction was associated with a deformation of the square pyramidal coordination sphere in this system. Investigation of the photophysical properties of these ligands revealed that only the reduced species **3** gave the solvent-dependent bimodal emission indicative of proton transfer-related emission pathways in the excited state, while the more acidic hydrazone **1** and Schiff base **2** exhibited more straightforward emission behaviour which was independent of solvent. These results outline a new path to a diverse family of functional heterotopic ligands for coordination polymers and MOFs, with 7AI-containing systems expected to offer useful inner-sphere

hydrogen bonding capabilities alongside a potential fluorescent signalling mechanism which may be linked to the electronic environment of the adjacent proton.

SUPPLEMENTARY MATERIAL

Additional data and information are available electronically at the pages of journal website: https://www.shd-pub.org.rs/index.php/JSCS/article/view/12451, or from the corresponding author on request. CCDC 2269543-2269546.

Acknowledgements. The authors gratefully acknowledge the Royal Society of Chemistry (Research Enablement Grant E21-4110373157) and the School of Chemical and Physical Sciences at Keele University for funding support. C.S.H. also acknowledges the X-ray diffraction group at the University of Novi Sad for fruitful discussions in Schiff base chemistry, facilitated by the Erasmus+ and Science Fund of the Republic of Serbia PROMIS schemes.

ИЗВОД

ЛИГАНДИ СА 7-АЗАИНДОЛНОМ ФУНКЦИОНАЛНОМ ГРУПОМ ЗА ФОРМИРАЊЕ ВОДОНИЧНИХ ВЕЗА У УНУТРАШЊОЈ СФЕРИ: СТРУКТУРНА И ФОТОФИЗИЧКА ИСПИТИВАЊА

ALEC B. COLES, OSKAR G. WOOD и CHRIS S. HAWES

School of Chemical and Physical Sciences, Keele University, Keele ST5 5BG, United Kingdom

У овом раду описана је синтеза, структурна анализа и спектроскопска карактеризација три нова 7-азаиндолна лиганда, као и новог координационог полимера са једним од ових лиганада, а са циљем идентификације нових мостовних лиганада са водоник-донорним групама у унутрашњој сфери. Структурна карактеризација је показала да 7-азаиндоли имају бољу водоник-донорну способност у хидразонској и иминској форми (једињења **1** и **2**), у поређењу са аминском (**3**). Насупрот томе, обрнути тренд је опажен када је испитивана водоник-акцепторска способност ових једињења. Ова сазнања се рефлектују и у резултатима флуоресцентне спектроскопије, који показују бимодалну емисију карактеристичну за присуство више хемијских врста које учествују у трансферу протона. Овај ефекат је присутан код амина, али не и код киселијих имина. У структури полимерног комплекса бакра(II) са хидразинским лигандом **1** уочено је очекивано формирање водоничних веза у унутрашњој сфери са сличном јачином као у слободном лиганду, што доводи до деформације координационе сфере. Ови резултати показују раније неиспитивану разноликост 7-азаиндолне функционалне групе као блока за изградњу лиганада у координационим полимерима и другим полинуклеарним врстама, са потенцијалом за стабилизацију путем водоничног везивања и интересантним фотофизичким својствима.

(Примљено 23. јуна; ревидирано 10. јула; прихваћено 8. септембра 2023)

REFERENCES

1. Z. Yin, Y.-L. Zhou, M.-H. Zeng, M. Kurmoo, *Dalton Trans.* **44** (2015) 5258 (https://doi.org/10.1039/C4DT04030A)
2. B. G. Diamond, L. I. Payne, C. H. Hendon, *Commun. Chem.* **6** (2023) 67 (https://doi.org/10.1038/s42004-023-00863-z)
3. M. Eddaoudi, J. Kim, N. Rosi, D. Vodak, J. Wachter, M. O'Keeffe, O. M. Yaghi, *Science* **295** (2002) 469 (https://doi.org/10.1126/science.1067208)

4. M. M. Radanović, S. B. Novaković, M. V. Rodić, L. S. Vojinović-Ješić, C. Janiak, V. M. Leovac, *J. Serb. Chem. Soc.* **87** (2022) 1259 (https://doi.org/10.2298/JSC220613072R)
5. P. D. Frischmann, V. Kunz, F. Würthner, *Angew. Chem. Int. Ed.* **54** (2015) 7285 (https://doi.org/10.1002/anie.201501670)
6. J. G. Betancourth, J. A. Castaño, R. Visbal, M. N. Chaur, *Eur. J. Org. Chem.* **2022** (2022) e202200228 (https://doi.org/10.1002/ejoc.202200228)
7. V. M. Leovac, V. S. Jevtović, L. S. Jovanović, G. A. Bogdanović, *J. Serb. Chem. Soc.* **70** (2005) 393 (https://doi.org/10.2298/JSC0503393L)
8. A. Erxleben, *Inorg. Chim. Acta* **472** (2018) 40 (https://doi.org/10.1016/j.ica.2017.06.060)
9. J.-F. Ayme, J. E. Beves, C. J. Campbell, D. A. Leigh, *J. Am. Chem. Soc.* **141** (2019) 3605 (https://doi.org/10.1021/jacs.8b12800)
10. S. Shaw, J. D. White, *Chem. Rev.* **119** (2019) 9381 (https://doi.org/10.1021/acs.chemrev.9b00074)
11. V. M. Leovac, M. V. Rodić, L. S. Jovanović, M. D. Joksović, T. Stanojković, M. Vujčić, D. Sladić, V. Marković, L. S. Vojinović-Ješić, *Eur. J. Inorg. Chem.* **2015** (2015) 882 (https://doi.org/10.1002/ejic.201403050)
12. A. Ferguson, M. A. Squire, D. Siretanu, D. Mitcov, C. Mathonière, R. Clérac, P. E. Kruger, *Chem. Commun.* **49** (2013) 1597 (https://doi.org/10.1039/C3CC00012E)
13. L. Fabbrizzi, *J. Org. Chem.* **85** (2020) 12212 (https://doi.org/10.1021/acs.joc.0c01420)
14. C. S. Hawes, *Dalton Trans.* **50** (2021) 6034 (https://doi.org/10.1039/D1DT00675D)
15. X.-L. Lv, S. Yuan, L.-H. Xie, H. F. Darke, Y. Chen, T. He, C. Dong, B. Wang, Y.-Z. Zhang, J.-R. Li, H.-C. Zhou, *J. Am. Chem. Soc.* **141** (2019) 10283 (https://doi.org/10.1021/jacs.9b02947)
16. K. Wang, Q. Wang, X. Wang, M. Wang, Q. Wang, H.-M. Shen, Y,-F. Yang, Y. She, *Inorg. Chem. Front.* **7** (2020) 3548 (https://doi.org/10.1039/D0QI00772B)
17. T. Basu, H. A. Sparkes, M. K. Bhunia, R. Mondal, *Cryst. Growth Des.* **9** (2009) 3488 (https://doi.org/10.1021/cg900195f)
18. C. S. Hawes, B. Moubaraki, K. S. Murray, P. E. Kruger, D. R. Turner, S. R. Batten, *Cryst. Growth Des.* **14** (2014) 5749 (https://doi.org/10.1021/cg501004u)
19. M. R. Healy, J. W. Roebuck, E. D. Doidge, L. C. Emeleus, P. J. Bailey, J. Campbell, A. J. Fischmann, J. B. Love, C. A. Morrison, T. Sassi, D. J. White, P. A. Tasker, *Dalton Trans.* **45** (2016) 3055 (https://doi.org/10.1039/C5DT04055H)
20. O. G. Wood, C. S. Hawes, *CrystEngComm* **24** (2022) 8197 (https://doi.org/10.1039/D2CE01475K)
21. R. S. Moog, M. Maroncelli, *J. Phys. Chem.* **95** (1991) 10359 (https://doi.org/10.1021/j100178a023)
22. X.-F. Yu, S. Yamazaki, T. Taketsugu, *J. Chem. Theory Comput.* **7** (2011) 1006 (https://doi.org/10.1021/ct200022a)
23. D. E. Folmer, E. S. Wisniewski, S. M. Hurley, A. W. Castleman Jr. *Proc. Natl. Acad. Sci. U.S.A.* **96** (1999) 12980 (https://doi.org/10.1073/pnas.96.23.12980)
24. A. V. Smirnov, D. S. English, R. L. Rich, J. Lane, L. Teyton, A. W. Schwabacher, S. Luo, R. W. Thornburg, J. W. Petrich, *J. Phys. Chem., B* **101** (1997) 2758 (https://doi.org/10.1021/jp9630232)
25. E. Wong, J. Li, C. Seward, S. Wang, *Dalton Trans.* (2009) 1776 (https://doi.org/10.1039/B814393E)
26. A. Domínguez-Martín, M. P. Brandi-Blanco, A. Matilla-Hernández, H. El Bakkali, V. M. Nurchi, J. M. González-Pérez, A. Castiñeiras, J. Niclós-Gutiérrez, *Coord. Chem. Rev.* **257** (2013) 2814 (https://doi.org/10.1016/j.ccr.2013.03.029)

27. B. Morzyk-Ociepa, K. Szmigiel, R. Petrus, I. Turowska-Tyrk, D. Michalska, *J. Mol. Struct.* **1144** (2017) 338 (https://doi.org/10.1016/j.molstruc.2017.05.059)
28. T. Steiner, *Acta Crystallogr., B* **57** (2001) 103 (https://doi.org/10.1107/S0108768100014348)
29. Y. Chen., R. L. Rich, F. Gai, J. W. Petrich, *J. Phys. Chem.* **97** (1993) 1770 (https://doi.org/10.1021/j100111a011)
30. P. Doungdee, S. Sarel, N. Wongvisetsirikul, S. Avramovici-Grisaru, *J. Chem. Soc., Perkin Trans. 2* (1995) 319 (https://doi.org/10.1039/P29950000319)
31. M. C. Etter, J. C. MacDonald, J. Bernstein, *Acta Crytallogr., B* **46** (1990) 256 (https://doi.org/10.1107/S0108768189012929)
32. B. Morzyk-Ociepa, K. Dysz, I. Turowska-Tyrk, D. Michalska, *J. Mol. Struct.* **1101** (2015) 91 (https://doi.org/10.1016/j.molstruc.2015.08.003)
33. T. Beyer, S. L. Price, *J. Phys. Chem., B* **104** (2000) 2647 (https://doi.org/10.1021/jp9941413)
34. M. Nishio, *CrystEngComm* **6** (2004) 130 (https://doi.org/10.1039/B313104A)
35. H. Yokoyama, H. Watanabe, T. Omi, S. Ishiuchi, M. Fujii, *J. Phys. Chem., A* **105** (2001) 9366 (https://doi.org/10.1021/jp011245g)
36. H. Masui, S. Kanda, S. Fuse, *Commun. Chem.* **6** (2023) 47 (https://doi.org/10.1038/s42004-023-00837-1)
37. A. W. Addison, T. N. Rao, J. Reedijk, J. van Rijn, G. C. Verschoor, *J. Chem. Soc., Dalton Trans.* (1984) 1349 (https://doi.org/10.1039/DT9840001349)
38. G. Bartlett, I. Langmuir, *J. Am. Chem. Soc.* **43** (1921) 84 (https://doi.org/10.1021/ja01434a010)
39. C. A. Taylor, M. A. El-Bayoumi, M. Kasha, *Proc. Natl. Acad. Sci. U.S.A.* **63** (1969) 253 (https://doi.org/10.1073/pnas.63.2.253)
40. J. Konijnenberg, A. H. Huizer, C. A. G. O. Varma, *J. Chem. Soc., Faraday Trans. 2* **84** (1988) 1163 (https://doi.org/10.1039/F29888401163).